

Formation of Liesegang patterns: A spinodal decomposition scenario

T. Antal¹, M. Droz¹, J. Magnin¹, and Z. Rácz²

¹ *Département de Physique Théorique, Université de Genève, CH 1211 Genève 4, Switzerland.*

² *Institute for Theoretical Physics, Eötvös University, 1117 Budapest, Pázmány sétány 1/a, Hungary
(October 9, 2018)*

Spinodal decomposition in the presence of a moving particle source is proposed as a mechanism for the formation of Liesegang bands. This mechanism yields a sequence of band positions x_n that obeys the spacing law $x_n \sim Q(1+p)^n$. The dependence of the parameters p and Q on the initial concentration of the reagents is determined and we find that the functional form of p is in agreement with the experimentally observed Matalon-Packter law.

PACS numbers: 05.70.Ln, 64.60.Cn, 82.20.-w

Pattern-forming chemical, physical and biological processes are common in nature and patterns often emerge in the wake of a moving front [1]. In particular, when an electrolyte A diffuses into a gel containing another electrolyte B , the eventual formation of a rhythmic pattern of precipitate by the moving chemical reaction front is known as the *Liesegang phenomenon* [2,3]. The observed precipitation patterns usually consist of a set of bands or rings (depending on the geometry of the system) clearly separated in the direction perpendicular to the motion of the front. This phenomenon is believed to be responsible for many precipitation patterns such as e.g. the structure of agate rocks [3]. Although the Liesegang phenomenon has been studied for a century, the mechanisms responsible for these structures is still under discussion [4].

Most of the reproducible Liesegang patterns are characterizable by the following generic laws. First, the position of the n -th band x_n (measured from the initial interface of the reagents) is proportional to $\sqrt{t_n}$ where t_n is the time elapsed till the appearance of the band. This so-called *time law* [5] is a direct consequence of the diffusive nature of the dynamics. Secondly, the positions x_n of the bands usually form a geometric series (*spacing law* [6]):

$$x_n \xrightarrow{n \text{ large}} Q(1+p)^n \quad (1)$$

where $p > 0$ is called the spacing coefficient and Q is the amplitude of the spacing law. Finally, the width w_n of the bands have been observed to increase with n and to obey the *width law* [7], $w_n \sim x_n$.

Most of the detailed experimental observations concern the spacing law. It has been found that the spacing coefficient p is a nonuniversal quantity depending (among other parameters) on the experimentally controllable concentrations a_0 and b_0 of the outer (A) and inner (B) electrolytes. This dependence is expressed by the *Matalon-Packter law* [8,9]:

$$p = F(b_0) + G(b_0) \frac{b_0}{a_0} \quad , \quad (2)$$

where F and G are decreasing functions of their argument b_0 [10].

The task of theories is to explain the existence of patterns obeying the spacing law (1) and, on a more sophisticated level, to derive the Matalon-Packter law (2). The theoretical approaches proposed up to now can be divided into two categories. The first one contains the *ion-product supersaturation* type theories [11–13] where the outer and inner reactants turn directly into precipitate ($A + B \rightarrow D$) whenever their local concentration product is above a threshold q^* . The second category contains the *intermediate-compound* theories [14,15] which assume the existence of a species C ($A + B \rightarrow C \rightarrow D$). The C -s are produced in a reaction-diffusion front that moves through the system and the precipitation $C \rightarrow D$ takes place only if the local concentration c reaches some threshold value c^* . In the presence of D , the process continues until the concentration of C drops below another threshold d^* . The problem with these theories is that either they contain parameters such as e.g. d^* that are difficult to control experimentally and not easy to grasp theoretically, or they describe a detailed mechanism that is too complicated to deduce quantitative consequences such as the Matalon-Packter law. Our goal with this Letter is to describe the formation of Liesegang patterns in terms of a model that contains the basic mechanism of phase separation that underlies the band formation but, at the same time, simple enough so that quantitative predictions are readily made. In particular we show the existence of the spacing law, obtain the Matalon-Packter law with estimates of $F(b_0)$ and $G(b_0)$ and, furthermore, the b_0/a_0 dependence of the amplitude Q of the spacing law is also determined.

All the theories discussed above can produce the spacing law but the comparison with the Matalon-Packter law suggest that the intermediate-compound theories are clearly preferable [4]. Accordingly, we shall assume that the motion of the reaction-diffusion front and the dynamics of the C particles deposited by the front should be the main ingredients of a theory of Liesegang patterns. The dynamics of the $A + B \rightarrow C$ front has been solved so its motion and the production of C -s are well known [16]. Thus the new aspect of our theory is the model for the dynamics of C -s.

In our picture, the C -s are particles that can move only by diffusion due to the presence of the gel. There is an attractive interaction between the particles that induces aggregation at low enough temperatures and high enough densities. An easily understandable, spatially discretized version of the model is the following spin-1/2 kinetic Ising model with competing spin-flip and spin-exchange dynamics [17]. Empty and occupied lattice sites are associated with down and up spins, respectively. The initial state is empty (all spins are down) and the moving front flips the down spins at a given rate (Glauber dynamics [18]). The diffusion is described by a spin exchange process (Kawasaki dynamics [19]). The rates of exchanges are governed by a heat bath at temperature T with ferromagnetic couplings between the spins modeling the attraction among the C 's. The experimentally observed freezing of the emerging patterns implies that the corresponding dynamics takes place at a very low effective temperature. If this model represents the pattern forming process correctly then one expects the emergence of bands of up and down spins in the wake of the moving spin-flip front. In order to understand how the bands arise, let us consider the phase diagram of an Ising model depicted on Fig.1.

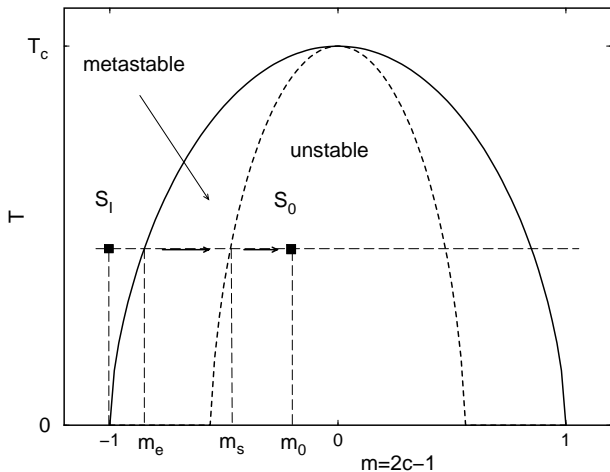


FIG. 1. Qualitative phase diagram for the Ising model. The magnetization m is related to the density c of C particles through $m = 2c - 1$. The solid line is the coexistence curve and the dotted one is the spinodal line. S_I is the initial state with $m = -1$, $\pm m_e$ are the equilibrium magnetizations at a given temperature T while $\pm m_s$ are the magnetizations at the spinodal line. The front alone would leave behind a magnetization m_0 .

One starts from the all-spins-down state (empty state, S_I in Fig.1). Since an $A+B \rightarrow C$ reaction front leaves behind a constant density c_0 of C -s [16], the spin-flip front is chosen such that it produces a local magnetization $m_0 = 2c_0 - 1$. We would like the front to bring the system into the unstable regime, thus $m_0 > m_s$ is assumed. As m is increasing from -1 to m_0 in the front, the local

state moves from S_I towards S_0 (Fig.1). With time, one crosses the coexistence line ($m = m_e$) and enters into the metastable phase [20]. Small clusters of up-spins nucleate at and aggregate behind the front. However, the nucleation is an activated process and so its characteristic time-scale τ_{nucl} is large at low temperatures. If τ_{nucl} is much larger than the time τ_{front} needed by the front to put out the local magnetization m_0 then the system reaches the unstable state i.e. crosses the spinodal line ($m = m_s$) [21]. Once the spinodal line is crossed, the phase separation takes place on a short time-scale and a spin-up domain is rapidly formed at or behind the front, hence the formation of a Liesegang band.

This band acts as a sink for the up-spins and, in the vicinity of the band, the local magnetization decreases and the front is no longer in the unstable region of the phase space. When the front moves far enough, the effect of the band as a sink diminishes. Thus the magnetization grows and the spinodal line is crossed again resulting in the formation of the next band. The repetition of this process should lead then to the Liesegang pattern. The new feature of the picture described above is the assumption that the state of the front is quasiperiodically driven into the *unstable* regime.

The above microscopic picture can be described on the mesoscopic level as follows. The diffusive dynamics of the coarse grained magnetization $m(x, t)$ is described by Model B of critical dynamics [22] with the moving spin-flip front appearing as a time-dependent source term $S(x, t)$:

$$\partial_t m(x, t) = -\lambda \partial_x^2 [\epsilon m(x, t) - \gamma m^3(x, t) + \sigma \partial_x^2 m(x, t)] + S(x, t) \quad (3)$$

where λ is a kinetic coefficient, ϵ measures the deviation from the critical temperature T_c and $\epsilon > 0$ ensures that $T < T_c$. The parameter γ is positive to guarantee overall stability and $\sigma > 0$ provides the stability against short-wavelength fluctuations. In principle, equation (3) should contain two noise terms. First, there should be thermal noise that, in the absence of the source, would bring the system to equilibrium described by the phase diagram in Fig.1. Second, there should be noise in the source S since the origin of this term is a reaction-diffusion process. We shall omit both noise terms. The thermal noise is neglected since the effective temperature is expected to be low as discussed above. As to the source term, it has been shown that the properties of the $A+B \rightarrow C$ type reaction fronts are mean-field like above dimension two [23]. We take this as an indication that the noise in S can be neglected.

In order to complete the description of the model, we need to discuss the actual form of the source term, S . The problem of the $A+B \rightarrow C$ reaction-diffusion front is well understood at the mean-field level [16]. The source term is the production rate of the C particles that can be calculated analytically. Provided the reagents A and B are

spatially separated at the initial moment [i.e. their densities are given by $a(x < 0, t = 0) = a_0$, $b(x < 0, t = 0) = 0$ and $a(x > 0, t = 0) = 0$, $b(x > 0, t = 0) = b_0$], the source term is a gaussian to an excellent accuracy:

$$S(x, t) = \frac{\mathcal{A}}{t^{2/3}} \exp \left[-\frac{[x - x_f(t)]^2}{2w^2(t)} \right]. \quad (4)$$

The center of the front moves as $x_f(t) = \sqrt{2D_f t}$ with the diffusion constant D_f given by the following equation $\text{erf}(\sqrt{D_f/2D}) = (a_0 - b_0)/(a_0 + b_0)$ with $D = D_a = D_b$ being the diffusion coefficient of the A and B particles [16,24].

The front is well localized since its width increases with a small power of time $w(t) = 2\sqrt{D}t^{1/6}/(ka_0K)^{1/3}$ where k is the reaction rate of the $A + B \rightarrow C$ process, and K is given by $K = (1 + b_0/a_0)(2\sqrt{\pi})^{-1} \exp(-D_f/D)$. Finally, the amplitude of the source can be expressed as $\mathcal{A} = 0.3ka_0^2K^{4/3}$. Thus the initial densities (a_0, b_0) , the diffusion constants $(D = D_a = D_b)$, and the reaction rate k determine all the parameters in $S(x, t)$ [16,24].

We turn now to the solution of eqn (3). In the absence of the source term, $S = 0$, the globally stable homogeneous solutions are $m_h^0 = \pm\sqrt{\epsilon/\gamma}$. One can also find other homogeneous solutions $m(x, t) = m_h$ which, however, are unstable to small perturbations if $|m_h| < \sqrt{\epsilon/(3\gamma)} = m_s$. The value m_s gives the location of the spinodal line [20].

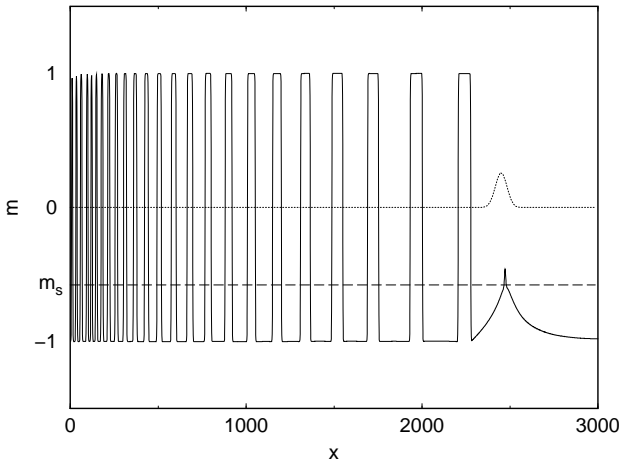


FIG. 2. Magnetization profile obtained for the following values of the front parameters: $D_f = 21.72$, $w_0 = 4.54$, and $\mathcal{A} = 0.181$ with length, time, and the magnetization (concentration) measured in units of $\sqrt{\sigma\epsilon}$, $\sigma/(\lambda\epsilon^2)$, and $\sqrt{\epsilon/\gamma}$, respectively. The dotted line denotes the rate of local magnetization increase due to the source, S , measured in units of $\lambda\epsilon^{5/2}/(\gamma^{1/2}\sigma)$ and magnified by a factor $2 \cdot 10^5$. The dashed line is the magnetization at the spinodal line, $m_s = -1/\sqrt{3}$.

In the presence of the source term S , equation (3) can be solved numerically using the initial condition $m(x, t) = -m_h^0$ and starting the source at the origin. The source alone would leave behind a uniform particle

density $c_0 \approx 0.85Ka_0\sqrt{D/D_f}$ [16] corresponding to a magnetization $m_0 = 2c_0 - 1$. The solution that evolves depends crucially on the value of m_0 .

If $|m_0| > m_s$, the system is always outside of the unstable domain and a uniform band of precipitate is formed. Since there is no noise in the system, this band is stable. Phase separation does take place when $|m_0| < m_s$ and a pattern similar to that shown in Fig.2 is observed. If m_0 is near the spinodal value then, at early stages of evolution, a nearly periodic set of narrow bands emerges that coarsens with time. Later on, the newly formed pattern crosses over to Liesegang type bands with the distance between consecutive bands increasing. If m_0 is such that the system is deep in the unstable domain, well defined Liesegang bands form from the very beginning (Fig.2 shows an example of this type of evolution).

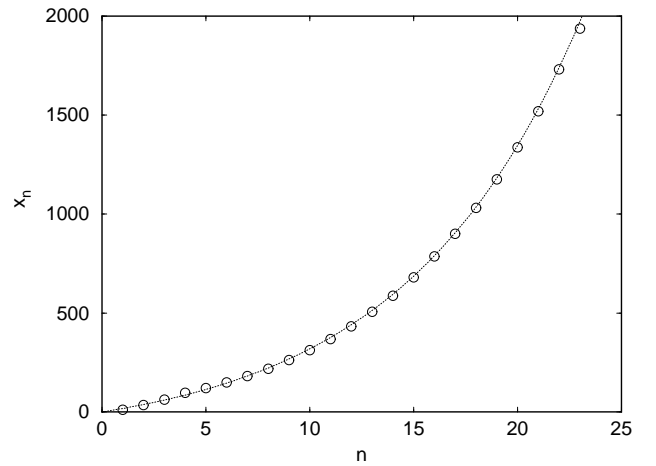


FIG. 3. Positions of the bands x_n as a function of their order of appearance n . Length is measured in units of $\sqrt{\sigma\epsilon}$. The full line is the best fit given by equation (5).

In agreement with experiments, once formed, the Liesegang type bands are static on the time-scale we are able to observe (occasionally up to 100 bands were generated). Thus their spacing is well defined and can be studied. Fig.3 displays the positions of the bands of the pattern exhibited in Fig.2. As one can see, a two-parameter fit of the form

$$x_n = Q[\exp(\tilde{p}n) - 1] \quad (5)$$

gives excellent agreement with the data (similar quality fits can be produced for a wide range of parameter values). Thus we see that the model contains the spacing law (1) with the spacing coefficient given by $1 + p = \exp(\tilde{p})$.

Next, one can investigate whether the patterns in our model obey the Matalon-Packter law. Calculating the p -s for a set of a_0 at a fixed b_0 , we find (see Fig.4) that the results indeed agree with the linear b_0/a_0 dependence given by eqn.(2). The slopes and the intersections with the p axis of the straight line fits provide us the functions

$F(b_0)$ and $G(b_0)$. Due to the restricted interval of b_0 values that are available we can deduce only an approximate functional form for these functions. It is clear, that both F and G are decreasing functions of their arguments, in agreement with experimental findings [8,9]. A fit to a power-law form gives $F(b_0) \sim b_0^{-1.7}$ and $G(b_0) \sim b_0^{-1.1}$.

From the point of view of applications, it is important to know the a_0 and b_0 dependence not only for p but also for the amplitude Q of the spacing law. In our model we can investigate this quantity as well and our preliminary results indicate that $Q(a_0, b_0) \sim (a_0/b_0)^{0.4}$. The increase of Q with a_0 is a somewhat surprising result. It means that, as far as the number of bands in a given interval is concerned, there is a competition between p and Q . When a_0 is increased, this number increases since $p \sim a_0^{-1}$ but it decreases due to the change in the amplitude $Q \sim a_0^{0.4}$. This means that in experiments where n is finite (typically $n \sim 20-30$) one could observe thinning of the bands as a result of the increase of the concentration of the outer electrolyte.

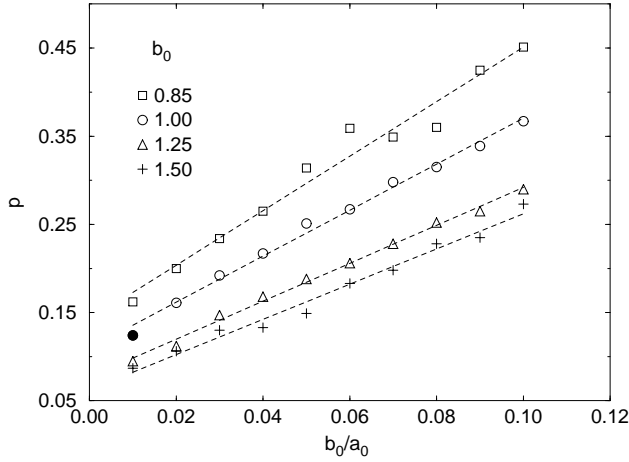


FIG. 4. Spacing coefficient p as a function of the ratio b_0/a_0 for several values of b_0 . The unit of b_0 is fixed by the considering the front parameters given in Fig.2 and setting $b_0/a_0 = 0.01$ (filled circle in this figure).

In conclusion we have proposed a new scenario for the formation of Liesegang patterns based on a spinodal decomposition mechanism. Our approach has the advantage of involving only a small number of parameters and there is no need to introduce artificial thresholds. Our model yields the Matalon-Packter law and allows the calculation of both the spacing coefficient $p(a_0, b_0)$ and the amplitude $Q(a_0, b_0)$ of the spacing law.

This simple scenario can be improved by studying the role of the noise either by adding it to the continuum model (3) or by carrying out Monte-Carlo simulations on the kinetic Ising model with competing dynamics as described above. Work along these lines is in progress [25].

ACKNOWLEDGMENTS

We thank M. Zrinyi, P. Hantz, and T. Unger for useful discussions. This work has been supported by the Swiss National Science Foundation and by the Hungarian Academy of Sciences (Grant No. OTKA T 029792).

-
- [1] M.C. Cross and P.C. Hohenberg, Rev. Mod. Phys. **65**, 851 (1994).
 - [2] R.E. Liesegang, Naturwiss. Wochenschr. **11**, 353 (1896);
 - [3] H. K. Henisch, "Periodic precipitation", Pergamon Press, (1991).
 - [4] For a recent comparison between theories and experiments see T. Antal, M. Droz, J. Magnin, Z. Rácz and M. Zrinyi, J. Chem. Phys. **109**, 9479-9486, (1998).
 - [5] Harry W. Morse and George W. Pierce: *Diffusion and Supersaturation in Gelatine*, Proceedings of the American Academy of Arts and Sciences, **38** 625-647 (1903)
 - [6] K. Jablczynski, Bull. Soc. Chim. France **33**, 1592 (1923).
 - [7] S. C. Müller, S. Kai, and J. Ross, J. Phys. Chem., **86**, 4078 (1982)
 - [8] R. Matalon and A. Packter, J. Colloid Sci. **10**, 46 (1955).
 - [9] A. Packter, Kolloid Zeitschrift **142**, 109 (1955).
 - [10] Note that the Matalon-Packter law is usually written in the form $p = F(b_0) + G(b_0)/a_0$. We altered the definition of G so that both F and G would be dimensionless.
 - [11] C. Wagner, J. Colloid Sci., bf 5, 85 (1950).
 - [12] S. Prager, J. Chem. Phys. **25**, 279 (1956).
 - [13] Ya .B. Zeldovitch, G.I. Barrenblatt and R.L. Salganik, Sov. Phys. Dokl. **6**, 869, (1962).
 - [14] G.T. Dee, Phys. Rev. Lett. **57**, 275 (1986).
 - [15] B. Chopard, P. Luthi and M. Droz, Phys. Rev. Lett. **72**, 1384 (1994); J. Stat. Phys. **76**, 661-676 (1994).
 - [16] L. Gálfi and Z. Rácz, Phys. Rev. **A38**, 3151 (1988).
 - [17] M. Droz, Z. Rácz, and J. Schmidt, Phys. Rev. **A39**, 2141 (1989).
 - [18] R.J. Glauber, J. Math. Phys. **4**, 294 (1963).
 - [19] K. Kawasaki, Phys. Rev. **145**, 224 (1966).
 - [20] J.D. Gunton, M. San Miguel and P.S. Sahni, *The dynamics of first order transitions*, in *Phase transition and Critical Phenomena*, Vol. 8, Ed. by C. Domb and J.L. Lebowitz, Academic Press (1983).
 - [21] The spinodal line is defined in equilibrium mean-field theories as the line where system becomes unstable. Otherwise it is a concept associated with the given dynamics in the system: It is the line where the linearized dynamical equations become unstable. We shall use the latter definition.
 - [22] P.C. Hohenberg and B.I. Halperin, Rev. Mod. Phys. **49**, 435 (1977).
 - [23] S. Cornell and M. Droz, Phys. Rev. Lett. **70**, 3824, (1993)
 - [24] The case of unequal diffusion coefficients can also be treated. See Z. Koza, J. Stat. Phys, **85**, 179 (1996).
 - [25] T. Antal, M. Droz, J. Magnin and Z. Rácz, unpublished.